

Hardware realization of test section walls of transonic wind tunnels on the basis of theoretical analysis and experimental research

Borivoj Blizanac, PhD (Eng)¹⁾

The accent is on the interference of wind tunnel test section walls and its elimination. The interference resulting from test section walls must be eliminated by these same walls in order to achieve conditions of free flight on their surfaces. The analytical calculation of the interference that has to be eliminated by partially open walls is impossible because of an extremely local character of the air flow in the vicinity of perforated walls, i.e. very high influence of viscosity effects in this range. The paper shows some of the most important and most interesting research efforts, mostly performed in wind tunnels of the first and second generation, from the aspect of obtaining an optimum geometry wind tunnel test section walls.

Ključne reči: transonic wind tunnel, test section, walls.

Used acronyms and symbols

M	- Mach number
M_∞	- Mach number of undisturbed air flow
q_∞	- Dynamic pressure of undisturbed airflow
θ	- Angle of airstream through perforated walls
K	- Pressure drop coefficient
K_p	- Perforated wall permeability coefficient
$\frac{\Delta p}{q_\infty}$	- Total pressure drop through the perforated wall
R_e	- Reynolds number
v_s	- Average vertical velocity in the slit open surface
v_∞	- Velocity of undisturbed airflow in the test section
p_∞	- Static pressure of undisturbed airflow in the test section
d_o	- Perforation-slit diameter
t	- Perforated wall thickness
Γ	- Circulation
l	- Elementary wing chord
δ	- Boundary layer thickness

Introduction

THE interference resulting from the wind tunnel test section walls must be eliminated by these same walls in order to achieve conditions of free flight over their surfaces. The analytical calculation of the interference that has to be eliminated by partially open walls is impossible to be performed because of an extremely local character of the air flow in the proximity of perforated walls, i.e. very high influence of viscosity effects at the distances close to the walls. Therefore, analytical expressions are just a rough picture of actual airflow conditions in subsonic as well as supersonic areas of air velocities. The theory of the two-dimensional incompressible flow, the linear theory of compressibility by Prandtl-Glauert in the subsonic flow, or the

method of characteristics in the supersonic flow, cannot be relevant for the determination of an optimum wall geometry for a total elimination of the interference of test section walls. The situation is even more delicate in the case of the airflow velocities close to the Mach number one, i.e. $M \approx 1$, where these theories are not applicable. However, this area is of particular importance in experimental aerodynamics because of well-known airflow phenomena. Therefore, this analysis should be taken as reference which can be relevant, only together with experimental support, for the development of the appropriate shape of the transonic wind tunnel walls.

It is of special interest to show some of the most interesting and most important research results, obtained in wind tunnels of the first and second generation, aimed to design optimum forms of the wall geometry. These results are mostly based on experimental work carried out by the AEDC research group with B. Goerth as a group leader, or based on his results published in the AGARDograph 49 of other research institutes [5].

Characteristics of the flow through partially open walls

Since the airflow characteristics are essentially linear, there is a linear dependence between the flow velocity and the pressure drop along the partially opened wall. This requirement has to be met not only by the flow streaming out of the test section, but also for the flow streaming into the test section from the test section chamber. The second condition is more difficult to fulfill because of the accumulated air with low kinetic energy in the test chamber. In that case air inflow can be implemented by the use of special wall configuration the geometry of which ensures adjustable wall resistance along that direction thus providing the necessary linear characteristics of the airflow.

¹⁾ Vidikovački venac 41, 11000 Beograd

The disturbances in the airflow occurring at the edges of each particular perforation have to be eliminated at a sufficiently short distance from the wall in order to prevent them to reach the model being examined. In order to meet this requirement, the perforations on the walls have to be of a sufficiently reduced size.

Thin perforated walls

As Pindzola showed [5], when the thin perforated wall is set at a high attack angle in the parallel stream (Fig.1), the induced pressure drop during the airflow is given by the following equation:

$$\frac{\Delta p}{q_\infty} = K_{\theta=90^\circ} \sin^2 \theta \quad (1)$$

where $K_{\theta=90^\circ}$ is the pressure drop coefficient ($\Delta p/q_\infty$) when the wall is set perpendicularly to the air stream ($\theta=90^\circ$).

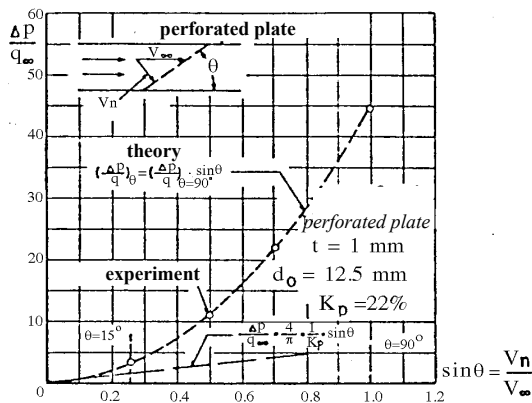


Figure 1. Pressure drop during the airflow through the perforated wall (Pindzola [5])

Experimental data are in excellent agreement with theoretical values given by the quadratic equation (1) for the values θ in the range $\theta=15^\circ \div 90^\circ$. However, the research in to $\theta < 15^\circ$, the most interesting angle range for transonic wind tunnels, has not been conducted yet. The geometrical characteristics of the walls in this experiment are: wall permeability coefficient $K_p=0.22$, perforation diameter 12.7 mm and wall thickness 1.02 mm.

When streaming angles are low, the elements of the rigid walls can be expected to behave as wing elements. This type of behavior of the thin perforated wall is even more obvious when an ideally perforated wall is replaced with a wall with a large number of perpendicular-transversal perforations. This wall behaves as a grid examined during the construction and development of compressors and turbines. At low streaming angles the grid produces lifting equivalent to the pressure drop along the wall and proportional to the attack angle. At higher attack angles of these grids, there is an additional pressure drop proportional to the square of the streaming velocity. In that case, the total pressure drop through the perforated wall can be given by the equation

$$\frac{\Delta p}{q_\infty} = K\theta + K_1\theta^2 \quad (2)$$

The linear term is usually sufficient to represent the behavior of perforated walls in wind tunnel experiments.

The agreement of the grid theory with the linear relation of the streaming coefficients can be expected only when the viscosity effects are not significant.

In the case of the increase of boundary layer thickness along the perforated walls, there are large deviations from the linear law. These deviations are equivalent to the behavior of the isolated wing for a low Reynolds number when the boundary layer increases on the wing surfaces.

Maeder [5] has analyzed a potential stream for a thin wall with one isolated transversal perforation-gap. In this simplified calculation, he proposed the following equation for the pressure drop during airflow

$$\frac{\Delta p}{q_\infty} = \frac{4 v_s}{\pi v_\infty} \quad (3)$$

where v_s is the average vertical velocity inside the open surface area of the gap.

The pressure drop during the incompressible flow, obtained by the previous equation, can be corrected for the compressible subsonic flow by using the linearized Prandtl-Glauert theory. In that case it can be written

$$\frac{\Delta p}{q_\infty} = \frac{1}{(1-M^2)^{1/2}} \frac{4 v_s}{\pi v_\infty} \quad (4)$$

According to this equation, the pressure drop along the gap (slit) increases by increasing the Prandtl factor, $1/(1-M^2)^{1/2}$. This relationship is valid neither for the Mach numbers close to one nor for considerable viscosity effects. The gap width has to be substantially larger than the thickness of the local boundary layer.

The same result can be obtained in the case of more than one transversal gaps if the distances between these gaps are longer than their width, i.e. if the ratio of the open surfaces of the wall, K_p , is low. The interaction between individual gaps is then negligible.

Eq.(4) can be also expressed in the form

$$\frac{\Delta p}{q_\infty} = \frac{1}{(1-M^2)^{1/2}} \frac{4}{\pi K_p} \theta \quad (5)$$

When the ratio of the open surfaces (of the wall) is relatively high, the interaction between individual gaps cannot be neglected, and the previous equations are not applicable any more. In that case, the wall with a number of transversal gaps can be analyzed as a grid, and each element of the wall between two gaps can be analyzed as a lifting surface. The grid in the parallel stream is shown in Fig.2.

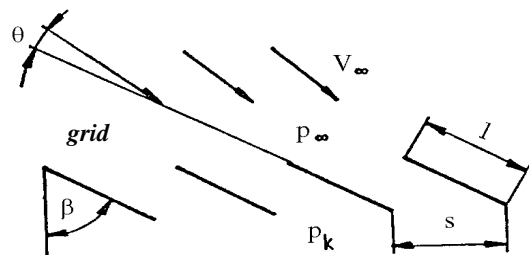


Figure 2. The grid in the parallel stream

The airflow characteristics were obtained for one turbine grid with eight lifting elements and the angle $\beta=90^\circ$, by Weining who used the conform projection. For that case, the lifting coefficient was given by eq.(6)

$$C_z = K_z 2\pi (\sin \theta_s) \left(\frac{v_{\infty s}}{v_\infty} \right)^2 \quad (6)$$

$$K_z = \frac{2}{\pi} \frac{1}{1-K_p} \operatorname{ctg} \left(\frac{\pi}{2} K_p \right) \quad (7)$$

with air circulation around each lifting element

$$\Gamma = v_{\infty s} l K_z \sin \theta_s \quad (8)$$

where l is a chord of the elementary wing. In these equations all terms with the subscript are related to the average conditions in the grid plane.

By applying similar laws of the incompressible aerodynamics, and after some transformations, Maeder defined the disturbing velocity in the direction of the airflow in the perforation plane

$$\frac{\Delta v_x}{v_\infty} = \sin \theta \operatorname{ctg} \left(\frac{\pi}{2} K_p \right) = K_p \frac{v_s}{v_\infty} \operatorname{ctg} \left(\frac{\pi}{2} K_p \right) \quad (9)$$

and the flow pressure drop along the wall

$$\frac{\Delta p}{q_\infty} = 2 \sin \theta \operatorname{ctg} \left(\frac{\pi}{2} K_p \right) = 2 K_p \frac{v_s}{v_\infty} \operatorname{ctg} \left(\frac{\pi}{2} K_p \right) = K \frac{v_s}{v_\infty} \quad (10)$$

where K is defined by eq.(11)

$$K = 2 K_p \operatorname{ctg} \left(\frac{\pi}{2} K_p \right) \quad (11)$$

For the compressible airflow, the factor K should be corrected by the Prandtl-Glauert factor $1/\sqrt{1-M^2}$. The results of these theoretical calculations are shown in Fig.3.

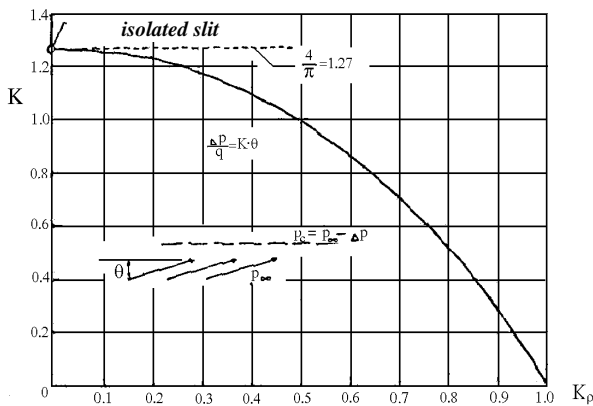


Figure 3. Pressure drop during airflow through the wall with transversal perforations according to the grid theory

The previous calculations were carried out for the air streaming through two-dimensional slits. For the perforated walls with different shapes of open surfaces, such as circular ones, the main physical aspects of the flow are the same as for the flow through the walls with perpendicular-transversal perforations. In this case, also, there are effects of the “attacking edge” on the low stream perforation border and effects of the “exiting edge” induced by the establishment of the “kutta” conditions on the intake perforation-gap border.

The elements of the wall between two open surfaces formed in this manner behave as wings with a low aspect ratio, and which, as already known, produce lower pressure drop than the walls with transversal slits (these ones behaving as wings with the infinite span).

In the supersonic flow field we can apply the analogy between the walls with perpendicular gaps and the perforated walls and thus obtain the flow parameters by using the method of characteristics and the theory of skew shock waves. The pressure drop through the wall with perpendicular-transversal gaps is

$$\begin{aligned} \frac{\Delta p}{q_\infty} &= \frac{2}{(M^2-1)^{\frac{1}{2}}} \left(\frac{1}{K_p} - 1 \right) \theta = \\ &= \frac{2}{(M^2-1)^{\frac{1}{2}}} (1-K_p) \frac{(\rho v)_s}{(\rho v)_\infty} = K \frac{(\rho v)_s}{(\rho v)_\infty} \end{aligned} \quad (12)$$

Because of the linearization of flow characteristics, this equation can be applied only for $M > 1$ (sufficiently higher). In the close proximity of the sonic velocity, the characteristics of a real flow lead to the definite value of K , instead of K approaching infinity.

Thick perforated walls

When the thickness of the perforated wall is larger than the diameter of the wall gap, individual elements of the wall do not behave as individual flanks of the grid anymore, which leads to considerable deviations in the behavior from the aforementioned airflow laws. Different types of partially opened walls of this type are shown in Fig.4.

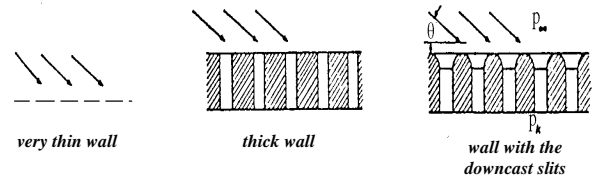


Figure 4. Different types of partially opened walls

In this case, airflow is similar to the flow through channels acting as diffusers and leading to the increase, instead of the decrease in pressure. These effects can particularly occur when each particular perforation is downcast and when branching of the air stream on the edges of perforations is avoided. The change in pressure for low airstream angles θ , (if the viscosity effects are neglected) can be given by eq.(13)

$$\frac{\Delta p}{q_\infty} = \frac{1}{K_p^2} \sin^2 \theta - 1 \quad (13)$$

where the minus sign shows that the pressure change is, in fact, the pressure increase.

From this equation it is clear that for thick perforated walls, the characteristics in pressure drop will not be that sloped as for the thin walls with the same geometry.

Transition boundaries between aerodynamically thin walls and acceptably thick ones cannot be determined just by theoretical considerations. Therefore, numerous systematic experimental research efforts were carried out in order to determine the optimum wall thickness, as well as other parameters of the wall geometry.

Experimental determination of the flow characteristics of perforated walls

For the confirmation and further development of the theory (of perforated wall flow characteristics) a large

number of experiments have been carried out. These experiments covered a large field of applicable wall geometry, in which different parameters were varied such as: wall thickness, size and orientation of the gaps, Mach number, etc.

The results of some of these experiments carried out in the first generation of wind tunnels will be given as illustration. These results confirm conclusions obtained by the theoretical analysis to a great extent.

Mclafferty [5] from the UNITED AIRCRAFT CORPORATION Laboratory, performed several series of experiments where he examined the influence of particular Mach numbers on the characteristics of the perforated wall flow. Typical results of such investigations are presented in Fig.5.

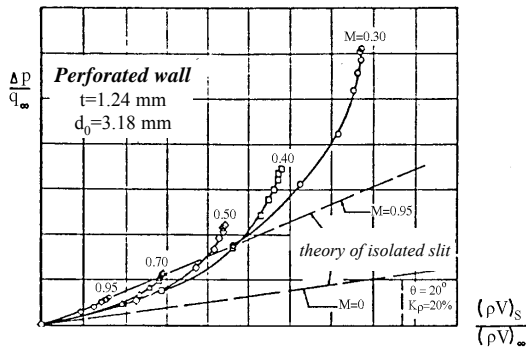


Figure 5. Characteristics of the airflow through the perforated wall at different subsonic Mach numbers [5]

The experimental data shown in Fig.5 were obtained under the following conditions: ratio of the open surfaces 7%, slit diameter $d_0=3.18$ mm and wall thickness $t=1.24$ mm. These results prove that the slope of the flow curve increases with the increase of the subsonic Mach number to an approximate value predicted by theory. The flow curves also show a pronounced tendency to deviate from linearity with the flow velocity increase. Furthermore, at each Mach number, the slopes of the curves become steeper at higher flow velocities, which means that at these higher velocities there is a sharp increase in flow resistance, i.e. airflow "suffocation" (obstruction). This suffocation occurs at relatively high flow velocities, i.e. at high flow angles θ .

For wind tunnel testing the most interesting range of flow angles is $\theta \leq 5^\circ$ approximately. In this range, airflow obstruction does not occur, and therefore there are no huge discrepancies between measured and theoretically expected values. This range of flow angles, the most interesting one, has not been examined thoroughly.

Another series of experimental tests, along with theoretical analysis, has been conducted for the Mach numbers $M=0.6 \div 1.24$, by Hill from the UNITED AIRCRAFT CORPORATION. For these experiments the conditions were: ratio of the open surfaces 7%, slit diameter $d_0=1.52$ mm and wall thickness $t=1.60$ mm.

It can be also seen that with the increase of the Mach number the slopes of the flow characteristics increase as well. There is also a very good agreement between experimentally obtained values and the theoretically predicted flow characteristic for $M=0.6$ and for an individual slit.

$$\frac{\Delta p}{q_\infty} = \frac{4}{\pi} \frac{1}{(1-M^2)^{\frac{1}{2}}} \frac{(\rho V)_s}{(\rho V)_\infty} \quad (14)$$

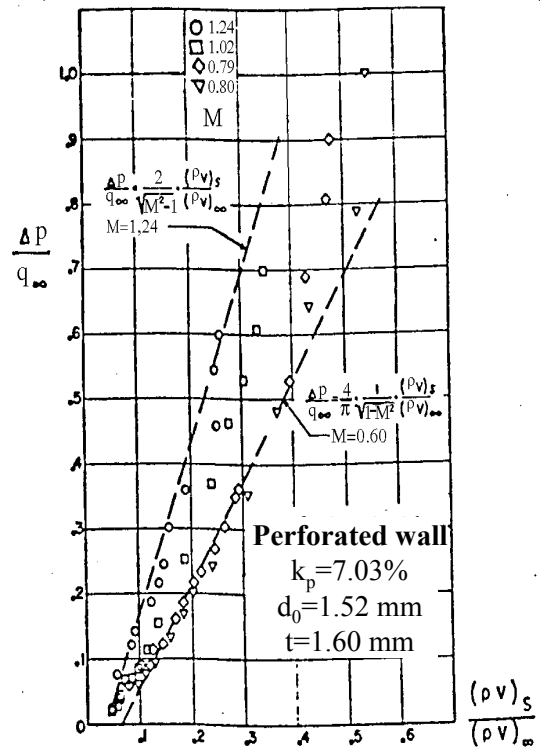


Figure 6. Characteristics of the airflow through the perforated wall at subsonic, sonic and supersonic flow velocities [3]

For $M=1.24$ (supersonic velocity) the measured curve is also in good agreement with a theoretically predicted slope

$$\frac{\Delta p}{q_\infty} = \frac{2}{(M^2 - 1)^{\frac{1}{2}}} \frac{(\rho V)_s}{(\rho V)_\infty} \quad (15)$$

Both assumptions introduced in theoretical considerations are completely justified since the ratio of open surfaces was relatively low 7%, i.e. the agreement with theory for individual slits for $M=0.6$ and $M=1.24$ by substituting the $(1-K_p) \approx 1$ in eq.(12) was experimentally verified.

In the previous experiment, the airflow direction was not inclined, but parallel to perforated walls so that the equation for the airflow pressure drop had to be modified (corrected) according to the difference between experimental and theoretical treatment for the inclined supersonic airflow. However, because of the low ratio of open surfaces for the examined wall, the difference between inclined and parallel airflows is rather small (not significant). In the previous experiments there is also an increasing curvature of the characteristic curves in the range of lower flow velocities, which is undoubtedly a consequence of the air viscosity effects. At higher flow velocities the boundary layer is more thoroughly sucked out through perforated walls. In that case, there is a better agreement between theory and experiment.

A general conclusion from the previously shown experimental data concerning the determination of the flow characteristics through perforated walls, is that the walls generally behave according to the theoretical model- theoretical analysis. However, this linearized theory of airflow can predict wall characteristics only when the boundary layer is thin and for small thickness of perforated walls when compared to the gap diameter. Additionally, average flow velocities have to be sufficiently lower than the flow velocities that lead to the air flow suffocation (obstruction).

Defining the geometry of perforated walls of the wind tunnel test section

In order to obtain optimum characteristics for the airflow through perforated walls, it is necessary to perform the analysis of the influence of the wall geometry on these characteristics, together with the analysis of the influence of flow parameters, i.e. Mach number and boundary layer thickness, on the wall geometry.

In other words, the analysis should include parameters such as: wall thickness, slit size, Mach number, boundary layer thickness, disturbance in airflow originated from wall slits, etc. Because of a very complex relationship between these flow and geometric parameters, an analytical determination of a detailed wall geometry is not possible.

A solution has been found in the experimental analysis performed in the first and second generation of transonic wind tunnels. The systematic experimental approach to these problems conducted by Goethert's [5] research group from the AEDC is among the most important ones.

The influence of the wall thickness

Fig.7 shows the results of an airflow behavior, under the following conditions: ratio of the open surfaces 22.5%, constant slit diameter $d_0=6.35$ mm, different wall thickness (changed in the range $t=1.59-25.4$ mm). The testing also included the change of the Mach number in all three velocity ranges, i.e. $M=0.75, 0.9, 1.0$ and 1.175 . It is clear from these measurements that the agreement between measured and theoretical flow curves for subsonic Mach numbers is much better in the case of relatively thin walls than in the case of relatively thick walls. Thin walls also have a significantly higher flow resistance coefficient.

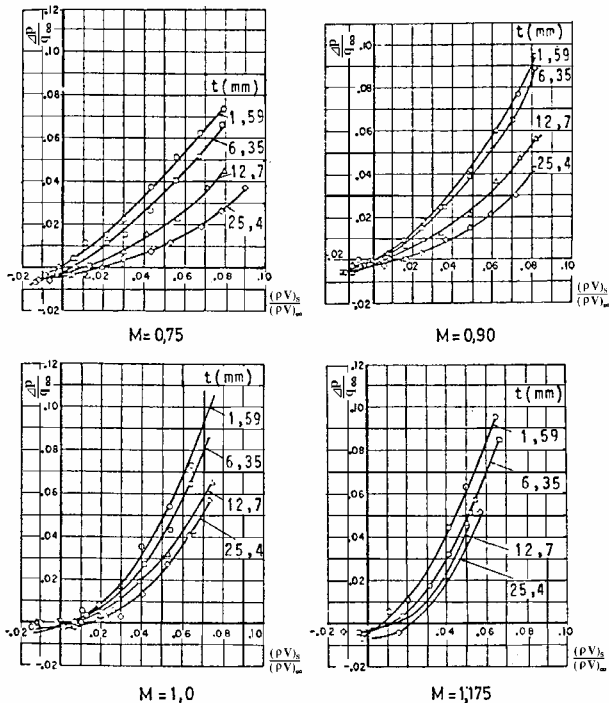


Figure 7. Influence of the wall thickness on the airflow characteristics for different Mach numbers [5]. Open surface ratio – 22.5% and constant slit diameter – 6.5 mm.

As seen from previous results, the boundary between aerodynamically thin and acceptably thick walls is $t=6.35$ mm, in other words, the value which is equal to the slit diameter, d_0 . This is in accordance with theoretical considera-

tions, since only the thin wall can behave as a series of individual flanks producing a desired pressure drop during the airflow.

At supersonic Mach numbers the influence of the wall thickness is not that clear as at subsonic Mach numbers. In both airflow velocity regimes, i.e. subsonic and supersonic, airflow curve properties display a significant deviation from the linear law for low flow ratios, $(\rho v)_s/(\rho v)_\infty < 0.04$, whereas for ratios higher than 0.04 airflow properties follow the linear law to a great extent. The deviation from the linear law for low flow ratios is explained by the influence of the boundary layer thickness. At higher flow velocities the suction of the boundary layer through the wall slits is more complete, which leads to linear flow characteristics. It should be emphasized that all the values of flow parameters are average values and that all the measurements are carried out at several positions along the wind tunnel test section. Only the average values of the pressure drop, $\Delta p/q_\infty$ and flow ratios, $(\rho v)_s/(\rho v)_\infty$ are shown in Fig.7.

The following conclusions can be drawn out of these experiments: the thickness of the perforated wall should not be greater than the diameter of the wall slits, d_0 , and the wall thickness also depends on the size of the test section.

The influence of the perforation size

Experimental data from the AEDC (Fig.8) shows that airflow properties are almost independent of the wall geometric parameters in the whole area of the mass flow ratio,

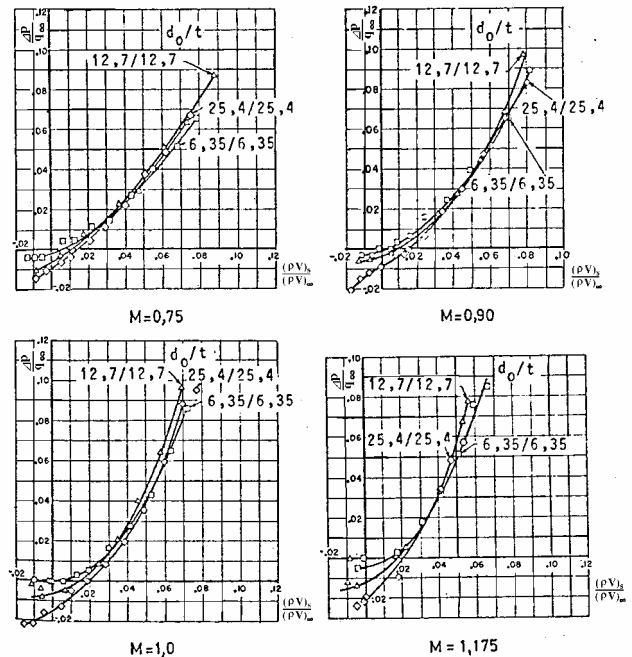


Figure 8. Influence of the slit size on the airflow characteristics for different Mach numbers. Opened surface ratio – 22.5%, and the same ratio between the slit diameter and the wall thickness in all measurements [5]

$(\rho v)_s/(\rho v)_\infty$ in all three velocity regimes, for a constant ratio of slit diameters and wall thicknesses, $d_0/t \left(\frac{1.59}{6.35}; \frac{6.35}{6.35}; \frac{12.7}{6.35}; \frac{25.4}{6.35} \right)$. This implies that it is possible to achieve the same flow effects for different slit diameters, but only when $d_0/t=1$. However, this is not true for small mass flows, when $(\rho v)_s/(\rho v)_\infty < 0.02$, and with expressed curvilinearity and dissipation of flow curves. The

able to achieve the same flow effects for different slit diameters, but only when $d_0/t=1$. However, this is not true for small mass flows, when $(\rho v)_s/(\rho v)_\infty < 0.02$, and with expressed curvilinearity and dissipation of flow curves. The

cause of this phenomenon is, again, the boundary layer effect, particularly in the case of small slit diameter sizes, $d_0=1.59$ and 6.35mm . The estimation of the smallest acceptable slit diameter of the perforated wall also depends on the boundary layer thickness and, according to the results given in [12], it can be determined from the condition that $d_0/2 > \delta$, where δ is the boundary layer displacement thickness. The determination of the acceptable upper limit of the slit-perforation diameter d_0 is closely connected with the size of the wind tunnel test section and with the uniformity of the flow field inside the test section. This slit size upper limit is paramount for the determination of an optimum slit diameter because a uniform flow field is of crucial importance in wind tunnel testings.

Influence of the perforation orientation

When the slits on perforated walls are tilted along the direction of the flow stream, as in the case shown in Fig.9, the flow going out from the test section becomes undisturbed, and the flow streaming into the test section much more obstructed. The airflow effects in the case of this type of perforated walls with a moderate thickness, t , are more similar to the airflow effects in the case of thin walls (for which airflow properties are much more linear in the whole range) than to the airflow effects in the case of walls of the same thickness but with slits perpendicular to the wall surface.

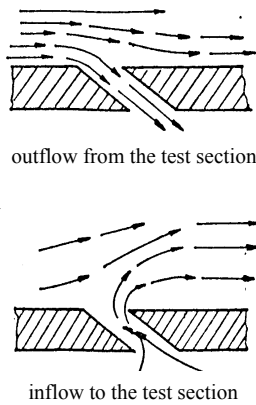


Figure 9. Shape of the airflow contour during air influx and efflux from/to the test section through the perforated wall with tilted slits

Systematic tests performed in the AEDC [5] for perforated walls with circular slits (the ratio of open surfaces 12%, slit diameter and wall thickness 6.35 mm, for different slit tilt angles 0° , 30° , 45° and 60°) indicate that at higher slit tilt angles the resistance for the outflow in the streaming direction is half the value of the flow resistance for lower slit tilt angles.

The most interesting information from these tests is that characteristic curves show a pronounced increase in slope, i.e. increase in flow resistance, for low and negative flow ratios. This is even more pronounced in the case of a slit tilt angle of 60° . The same behavior of the flow curves was in the whole range of the tested Mach numbers, as shown in Fig.10 for two representative values of Mach numbers $M=0.9$ and $M=1.10$.

In addition to the previously mentioned advantages of the walls with tilted slits over the walls with perpendicular slits, i.e. easiness in achieving more linear flow characteristics, decreasing the outflow resistance and increasing the inflow resistance, another advantage of this type of perforations is a required lower ratio of open surfaces (i.e. the wall

permeability factor, K_p , defined by the total slit surface area measured perpendicularly to the slit tilt angle axis, in relation to the total wall surface area).

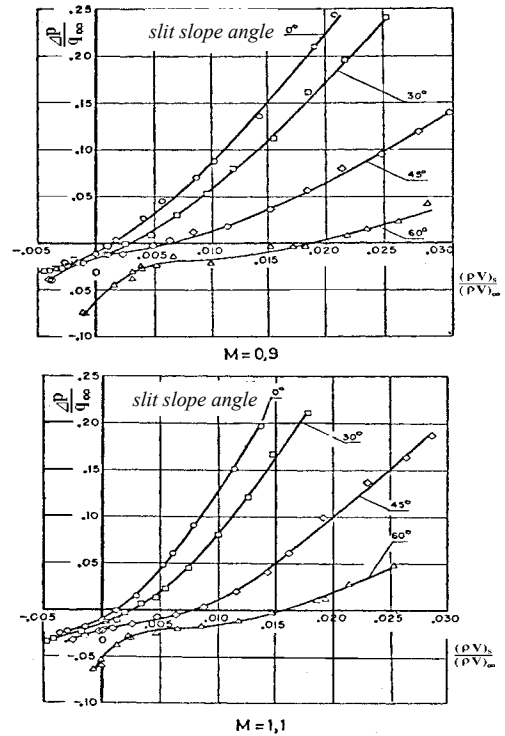


Figure 10. Influence of the slit orientation on airflow properties. Slit diameter and wall thickness – 6.35 mm, and the ratio of open surfaces – 12% [5].

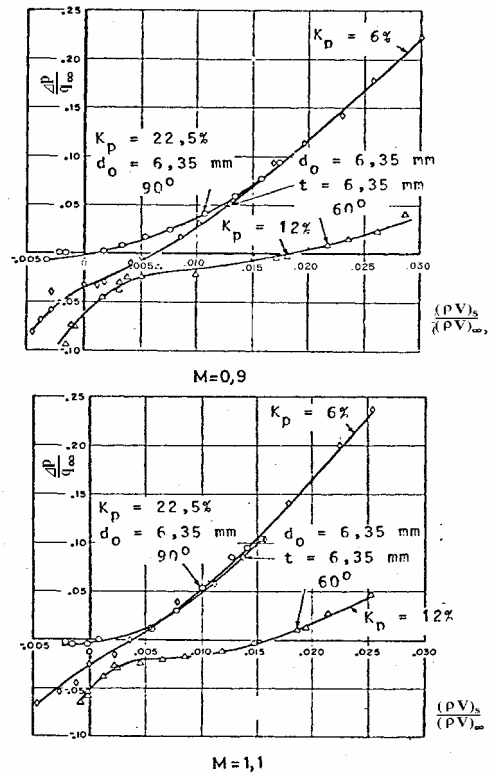


Figure 11. Comparison of the airflow characteristics for the perforated walls with perpendicular slits and for the walls with slits tilted 60° , for different values of open surfaces [5]

The experimental data analysis shown in Fig.11 indicates that the flow characteristics are practically identical for the same wall geometry (wall thickness and slit diameter of

6.35 mm), slit tilt angles of 0° and 60° , and for different ratios of open surfaces, 22.5% for perpendicular slits and 6% for perforations with a tilt angle of 60° .

Under the same geometric parameters, the wall with perforations-slits tilted 60° and the ratio of open surfaces of 6% behaves exactly the same as the wall with perpendicular perforations with the ratio of open surfaces of 22.5%. It is also clear that in both ranges of Mach numbers the linear flow characteristics have been achieved for tilted perforations and low mass flow ratios.

Tests regarding the influence of the slit size and wall thickness have also been performed in the AEDC [5]. In these tests, the previously mentioned conclusion that the optimum ratio between the slit diameter and the wall thickness is one has been confirmed for perpendicular as well as for tilted perforations.

The influence of the boundary layer thickness

In the previous discussion a very important effect of the boundary layer thickness on airflow characteristics has been emphasized. This influence is particularly pronounced at low and negative values of the mass flow ratio. In order to reduce this undesirable effect the AEDC research group performed the series of experiments to determine the conditions under which these effects occur place and possible resources for their elimination [5]. The experimental data from these tests are shown in Fig.12.

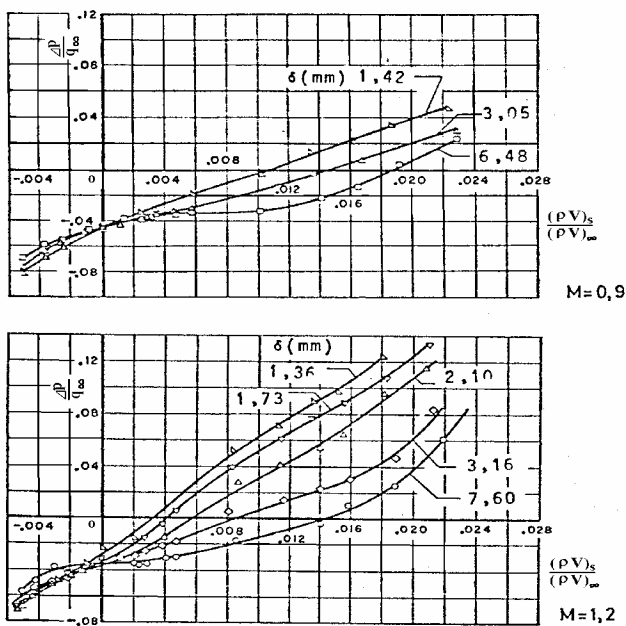


Figure 12. Influence of the boundary layer thickness on airflow characteristics for the perforated wall with slits tilted 60° , slit diameter 3.175 mm and the ratio of open surfaces 6%

The experimental data were obtained for the wall with the slits tilted 60° , with slit diameter and wall thickness of 3.175 mm and the ratio of the open surfaces 6%. As it can be seen from Fig.12, the flow characteristics show high irregularity in all cases when the boundary layer thickness was larger than the slit diameter of the perforated wall (Fig.12a). This is more pronounced in the supersonic velocity regime, where the boundary layer thickness should not exceed about 75% of the slit diameter (Fig.12b). For the walls with perpendicular slits this requirement is even more rigorous, and the boundary layer thickness should not exceed 50% of the slit diameter [12]. During these experi-

ments it was observed that in the case of the walls with tilted perforations there was a tendency of boundary layer formation with much more uniform thickness along the direction of the test section axis.

To reduce the boundary layer thickness on the test section perforated walls it is necessary to ensure a certain difference between the test section pressure and the pressure of the test section chamber. The easiest method to achieve this is by air suction and correct adjustment of the pressure in the test section chamber. This methodology enables establishing of almost linear flow characteristics at the transonic Mach number range. For the wall with perforations tilted 60° , gap diameter and wall thickness 3.125 mm and the ratio of open surfaces 6% this was experimentally confirmed for the range of Mach numbers $M=0.9 \div 1.4$. This is shown in Fig.13. At all Mach numbers the boundary layer thickness did not exceed 50% of the slit diameter, which means that air suction from the test section chamber was correctly implemented. The character of the flow curves has additionally proved it.

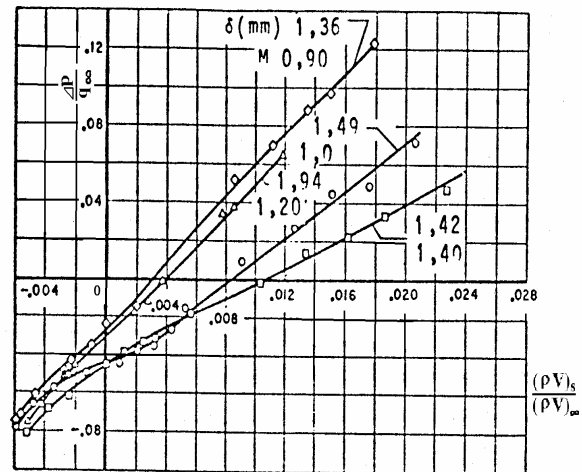


Figure 13. Influence of the Mach number on airflow characteristics for perforated walls with slits tilted 60° , slit diameter and wall thickness 3.125 mm, ratio of open surfaces 6% for a relatively thin boundary layer [5]

Influence of the perforation size on airflow properties

The influence of the size of wall perforations (coefficient K_p) on airflow characteristics, i.e. on the quality of the flow field in the test section, is not possible to be exactly defined mathematically because of very complex relation among a large number of geometric and airflow parameters. Comprehensive experimental studies [2], [5], [6], performed in the 1950s in the second and third generation of transonic wind tunnels, with special involvement of the AEDC research group [5], [2], made a very important contribution to further development of wind tunnels with adjustable perforations of test section walls [6]. In these studies the influence of slit angle tilting has been examined along with the studies of the influence of a model size (through the size of geometric blockage defined in percents as a ratio of the cross section of a studied model to the a wind tunnel test section surface). A study performed in the AEDC transonic wind tunnel, with the test section of a quadratic cross section ($1.2 \times 1.2 \text{ m}^2$) and adjustable perforations, $K_p=0 \div 10\%$, showed that, under a blockage of 1%, optimum results of pressure distribution on a conical model are obtained for particular values of the coefficient K_p and the Mach number. This dependence is shown in Fig.14.

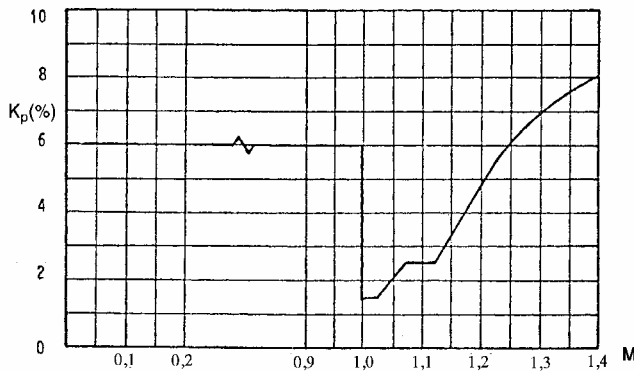


Figure 14. Optimum value for the perforation size as a function of the Mach number for the parallel wall with slits tilted 60° [6]

It is characteristic that the optimum perforation size is constant and equal to 6% in the subsonic range, whereas in the supersonic airflow field it is variable and ranges from 1.5% for $M=1$ to 8% for $M=1.4$. In this range of Mach numbers tests have been performed to establish the influence of the perforated wall tilt angle; i.e. converging walls with an angle of -0.5° to diverging ones with an angle of $+0.5^\circ$. The results gained from these experiments shed no light on the influence of the perforated wall tilt angle, neither they showed advantage over parallel walls.

Effects of the size of model geometric blockage are more clear after the AEDC experiments on slim (flexible) cylindrical models. In that case, blockage should not exceed about 3%. This value is conditional since it depends on the shape of a tested model.

Airflow disruption by the slits of test section perforated walls

Schlieren images of supersonic flow in the test section with perforated walls show that wall perforations generate many small waves in to the main air stream. These waves spread out over relatively large distances from the perforated wall. In a supersonic airstream each perforation generates compression and expansion waves which are mutually attenuated at a sufficiently large distance from the wall. The distance at which these waves are satisfactorily eliminated depends on the size and shape of the wall perforation and on the Mach number in the test section.

Numerous experiments have been conducted to establish pressure perturbations generated by the test section wall perforations. In the AEDC transonic model wind tunnel [5], tests included different types of perforated walls with perpendicular perforations, with the ratio of open surfaces 22% for parallel walls and for convergently positioned perforated walls with a convergence angle of 30° . Measurements were conducted in planes parallel to the walls at different distances from the walls and at different Mach numbers. Total uniformity in airflow was observed in planes very close to the walls at subsonic Mach numbers, whereas at supersonic Mach numbers uniformity was achieved only at some distances from the walls [5]. On the basis of these experiments, it is possible to draw some conclusions about the level of airflow uniformity as a function of the distance from the wall. The most suitable way is to express this airflow nonuniformity in the test section as a deviation in the Mach number $\Delta M = M - M_s$, i.e. deviation of the local Mach number from the average value (Fig.15). The diagram in Fig. 15a) shows that initial disturbances rapidly decrease at distances of approximately 24 perforation diameters, reaching the value of $\Delta M = 0.002$.

Similar experiments have been conducted for the test section walls with tilted perforations (tilt angle of 60°). The ratio of open surfaces was 6%. Parallel and convergent walls (convergence angle was 30°) of test section were tested in these experiments. The results of these experiments are shown in Fig.15b). From these results it can be concluded that initial disturbances reach a value of $\Delta M = 0.002$ for distances approximately equal to 30 average perforation diameters.

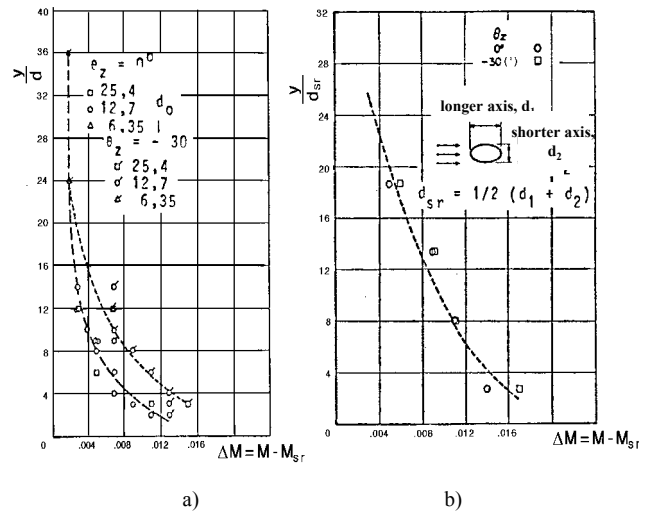


Figure 15. Attenuation of the airflow disturbance induced by different perforated walls for Mach number 1.25 [5]; (a) perpendicular slits; (b) slits tilted 60°

Therefore, a model should not be positioned at distances shorter than 30 perforation diameters. Since these results were obtained in a two-dimensional model transonic wind tunnel (with perforations on the top and bottom walls) where the boundary layer is much thicker than the boundary layer in wind tunnels with all four perforated walls, diameters of wall perforations should not exceed $1/80$ to $1/100$ of the test section height. Moreover, the lower acceptable limit for the perforation diameter (that depends on the boundary layer thickness) should not be smaller than a double value of the boundary layer thickness.

Influence of the Mach number

Experimental data in Fig.8 depict the influence of the Mach number on the airflow characteristics. It is clear that flow resistance decreases with the increases of the Mach number, i.e. suction of air is more efficient at larger Mach numbers. Airflow characteristics stay the same in all three flow velocity ranges in almost the whole range of flow mass ratios. This is very close to the theoretical case, i.e. linear dependence, except for low mass flow ratios $(\rho v)_s / (\rho v)_\infty < 0.02$. The deviation from the linear law and airflow curve dispersion in the range of low mass flows is characteristic for all Mach numbers and can be explained by the influence of the boundary layer. For these cases, the boundary layer at low suction rates is very thick. Therefore, this deviation is most pronounced in the case of small slit diameters $d_0 = 6.35$ (mm).

Hardver solutions for air suction from the test section chamber

A transonic airflow of required quality in the test section of transonic wind tunnels is possible to be obtained in several ways. They differ in a method of providing necessary

auxiliary air suction from the test section chamber. Some of available possibilities are graphically shown in Fig. 16.

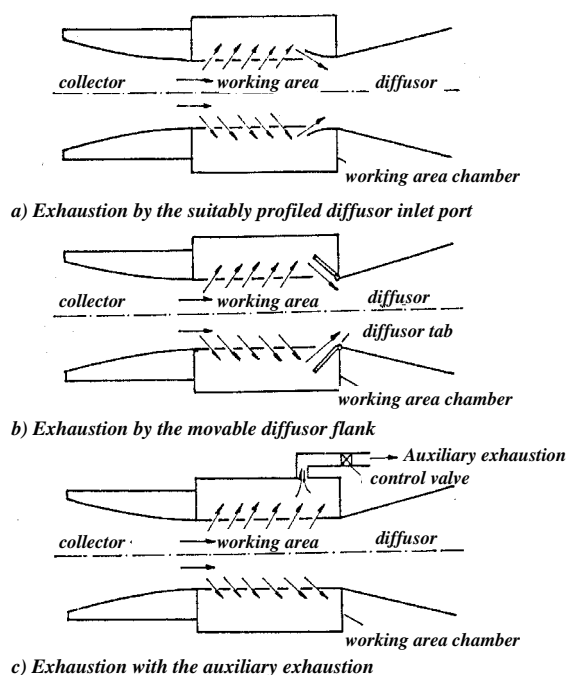


Figure 16. Different possibilities for air suction from the chamber of the wind tunnel test section

Besides construction simplicity, the first two possibilities (Fig. 16a),b)) have an additional advantage - no additional equipment is necessary for their operation. This is not the case for the option shown in Fig. 16c). However, the first two solutions have some serious disadvantages concerning the efficiency of operation and the possibility of adaptation to optimum conditions in the wind tunnel test section with the change of the Mach number, shape and the angle of attack of the model. This is particularly the case with the option shown in Fig. 16a). The construction solutions depicted in Fig. 16a) and 16b) belong to the past and are attributed to the first and second generation of transonic wind tunnels [1,2,4,8]. The third and fourth generations of transonic wind tunnels belong mostly to the type schematically presented in Fig. 16c), or to some of its modifications [6,7,8,9,10,11].

Conclusion

Since the characteristics of the airflow through partially opened walls of the wind tunnel test section are basically linear, there is a linear dependence between the airflow velocity and the pressure drop through partially opened walls. The linearity requirement has to be fulfilled not only for the air streaming out of the test section, but also for the air streaming into the test section chamber. The requirement

imposed by the second condition is much more difficult to fulfill, because of the accumulated air residue of a very low energy in the test section chamber. In that case, air streaming into the chamber can be implemented by a special configuration of the wall the geometry of which provides variable wall resistance in that direction. In that way it is possible to achieve airflow linear characteristics. Disturbances in the airflow occurring at the edges of each particular slit-perforation have to be eliminated at a sufficiently close distance from the wall in order to prevent them to reach the model being tested. As a consequence, these slits should be sufficiently small.

Experimental verification of the characteristics of the airflow through perforated walls has been given in this paper for a broad area of applicable wall geometry. The influence of different parameters, such as wall thickness, size and orientation of slits, Mach number, etc., has been discussed.

In order to acquire optimum characteristics of the airflow through perforated walls of the wind tunnel test section it is necessary to analyse the wall geometric parameters and their influence on the flow characteristics, as well as the influence of the flow parameters (Mach number, thickness of the boundary layer, etc.) on the wall geometry.

References

- [1] WRIGHT, R., WARD, V. *NACA Transonic wind tunnel test sections*, NACA Rep. 1231, 1955.
- [2] HOLDER, D., NORTH, R., CHINNECK, A. *Experiments with slotted and perforated walls in a two-dimensional high-speed tunnel*, A.R.C.R. and M. No. 2955, November 1956.
- [3] HEASLET, M., SPREITER, J. *Three-dimensional transonic flow theory applied to slender wings and bodies*, NACA Rep. 1318, 1957.
- [4] SIERIEIX, M. *Equipment transsonique des souffleries de recherche de l'O.N.E.R.A. La Recherche Aeronautique*, decembre 1958.
- [5] GOETHERT, B. *Transonic wind tunnel testing*. AGARDograph 49, Pergamon Press, New York, 1961.
- [6] JACOBS, J. *Determination of optimum operating parameters for the Aedc-pwt 4-ft transonic tunnel with variable porosity test section walls*. AEDC-TR-69-164, August, 1969.
- [7] RAINBIRD, W. *Design and use of boundary layer control for 2D Airfoils testing: NAE 15x60 In Section*. Memo. H SA-40, February, 1970.
- [8] OHMAN, L. *The NAE High Reynolds Number 15x60 In Two dimensional Test Facility*. Part I, General Information, NCR Report LTR-HA-4, April 1970.
- [9] SEARS, W. *Self-correcting wind tunnels*. *Aeronautical Journal*, Feb/March, 1974.
- [10] CHEVALLIER, J.P. *Parois auto-correctrices pour soufflerie transsonique*. 12^{eme} Colloque D'Aerodynamique Appliquee ENSMA/CEAT- POITERS, 5,6 et 7 novembre 1975.
- [11] SEARS, W., VIDAL, R., ERICKSON, J., RITTER, A. *Interference-free wind tunnel flows by adaptive-wall technology*. 10th Congress of the International Council of the Aeronautical Sciences ICAS, 4-8 October, 1976, Ottawa, Ontario, Canada.

Received: 15.10.2003

Hardverska realizacija zidova radnog dela transoničnih aerotunela na osnovu teorijske analize i eksperimentalnih istraživanja

U radu se stavlja naglasak na sopstvenoj eliminaciji interferencije zidova radnog dela aerotunela. Interferencija koja je nastala od samih zidova radnog dela aerotunela, mora se istim zidovima i eliminisati, kako bi se postigli uslovi slobodnog leta na njihovim površinama. Analitički proračun ove interferencije koju treba eliminisati parcijalno otvorenim zidovima je nemoguće izvesti, zbog izuzetno lokalnog karaktera strujanja u blizini perforiranih zidova, od-

nosno vrlo velikog uticaja viskoznih efekata u ovom domenu. Prikazana su neka od najznačajnijih i najinteresantnijih istraživanja koja su uglavnom izvršena na prvoj i drugoj generaciji aerotunela, sa stanovišta dobijanja optimalnih formi geometrije zidova radnog dela aerotunela.

Ključne reči: transonični aerotunel, zidovi radnog dela.

Réalisation de matériel des parois de la chambre d'expérience dans la soufflerie transsonique en partant de l'analyse théorique et les recherches expérimentales

L'interférence provenant de parois de la chambre d'expérience dans la soufflerie doit être éliminée par ces mêmes parois afin d'assurer les conditions du vol libre sur leur surface. Le calcul analytique de cette interférence qui doit être éliminée par les parois partiellement ouverts n'est pas possible à cause de la caractéristique extrêmement locale de l'écoulement près de parois perforés, c'est-à-dire à cause de très grands effets de viscosité dans ce domaine. Quelques-unes de recherches les plus importantes et les plus intéressantes, effectuées en souffleries de première et seconde génération pour la plupart de cas, sont présentées afin de trouver les formes optimales des parois de la chambre d'expérience.

Mots-clés: soufflerie transsonique, parois de la chambre d'expérience.